Automatika

Journal for Control, Measurement, Electronics, Computing and Communications

ISSN: (Print) (Online) Journal homepage: https://www.tandfonline.com/loi/taut20

Convolutional Neural Network-based harmonic mitigation technique for an adaptive shunt active power filter

K. R. Sugavanam, K. Mohana sundaram, R. Jeyabharath & P. Veena

To cite this article: K. R. Sugavanam, K. Mohana sundaram, R. Jeyabharath & P. Veena (2021) Convolutional Neural Network-based harmonic mitigation technique for an adaptive shunt active power filter, Automatika, 62:3-4, 471-485, DOI: 10.1080/00051144.2021.1985703

To link to this article: https://doi.org/10.1080/00051144.2021.1985703

Published online: 04 Oct 2021.

AUTOMATIKA
2021, VOL. 62, NOS. 3–4, 471–485
https://doi.org/10.1080/00051144.2021.1985703

Convolutional Neural Network-based harmonic mitigation technique for an adaptive shunt active power filter

K. R. Sugavanam [a], K. Mohana sundaram[b], R. Jeyabharath[c] and P. Veena[c]

[a]Jaya College of Engineering and Technology, Chennai, India; [b]KPR Institute of Engineering and Technology, Coimbatore, India; [c]K. S. R. Institute for Engineering and Technology, Tiruchengode, India

ABSTRACT

Owing to the use of nonlinear loads in the distribution side, there are power quality issues such as voltage swell/sag, harmonics, flickers, voltage imbalance, and outage. The harmonics in power system affect the quality of power and hence a suitable methodology is vital to mitigate the harmonics and compensation of reactive power. In this paper, CNN (Convolutional Neural Network)-based harmonic mitigation is performed. A 5-level cascaded H-bridge inverter is employed as a shunt active filter in which the reference current is generated by the SRF theory, incorporating CNN for harmonic extraction. The DC-link potential across capacitor is retained by means of ANN (Artificial Neural Network) controller whose behaviour is compared with a proportional controller as well as FLC. The gating pulse for the cascaded inverter is generated by means of PWM generator incorporated with Hysteresis Current Controller (HCC). By this control strategy, the harmonics in the current and voltage get mitigated; subsequently, the reactive power compensation is achieved with unity power factor. By implementing the five-level inverter, the THD and the settling time are minimized. The performance of the system is analysed using MATLAB for nonlinear load and the hardware is implemented with FPGA Spartan 6E. The THD of 0.93% is accomplished in simulation and 1.4% in the hardware execution.

ARTICLE HISTORY
Received 10 November 2020
Accepted 21 September 2021

KEYWORDS
SRF theory; shunt active filter; Hysteresis Current Controller; five-level cascaded inverter; Convolution Neural Network; Artificial Neural Network

1. Introduction

Power System faces many serious issues because of various disturbances that affect the quality of power, mainly because of the nonlinear loads applied in the domestic and industrial background. Some of the Power Quality (PQ) problems that affect the distribution side are voltage sag/swell, harmonics, flickers, outage, and voltage imbalance. Among these power system harmonics is a vital factor that affects the quality of power which occurs mainly because of the use of power electronic devices, variable speed drives, SMPS, arcing devices, etc. These can be rectified by evaluating the source of the issue [1,2]. SVC, STATCOM, and DVR are FACTS devices which are employed in mitigating the PQ disturbances, also controllers are incorporated with these devices to attain the ideal performance [3–5]. PQ problems, including harmonics, are achieved by means of passive or active filters. Usually, passive filters are employed for these problems, but for its large size and fixed compensation active filters are preferred [6,7]. In this paper, shunt active filter (SAF) is employed and several papers review the functioning of shunt active filters. Over damping performance can be achieved by adjusting the gain in shunt active filters is discussed in [8]. Adaptive shunt filter-based Artificial Neural Network that is introduced to reduce the harmonics in current for unbalanced load conditions is discussed in [9]. The performance of SAF with fluctuating supply potential provided a constant dc-link voltage is studied in [10]. A simple optimization algorithm without complex techniques introduced to mitigate the current harmonics with unity power factor is discussed in [11]. An adaptive controller, introduced for the proper working of shunt active filters to mitigate the harmonics for an unbalanced load condition, is discussed in [12]. A high crest factor is attained by a modular shunt active power filter, which reduces harmonics, is discussed in [13]. Compensation of reactive power and harmonics is carried out without transformer reducing the cost and size, as discussed in [14].

An ideal power circuit for the shunt active filters to mitigate harmonics is the use of Multi level inverters (MLI). Among the different topologies of MLI, the diode clamped topology produces more harmonics as there are a number of diodes, in the flying capacitor topology, there is unbalancing in the capacitor voltage. And so in this paper cascaded topology is chosen because the problem of voltage unbalances and the use of extra-clamping diodes is avoided. Several literatures discuss the use of multi-level inverters. A cascaded H-bridge MLI is introduced in [15], in which high power quality can be achieved by adding the number of volt-

CONTACT K. R. Sugavanam sugavanamkr@gmail.com

age levels. A control algorithm for detecting the harmonics developed for H-bridge 3-level inverter is discussed in [16]. To provide gating signal for the five-level inverter, modulation technique presented with minimized switches and driver circuits is discussed in [17]. A significant factor explains the number of modules per voltage level, as discussed in [18] which can be stretched for different voltage levels by including additional stages. Cascaded H-bridge 5-level inverter incorporated by means of a PID controller is established for controlling the capacitor potential with reduction in the size; cost and weight are achieved in [19]. Cascaded multi-level inverter, which regulates the quality of power delivered with minimized cost and space, is presented [20].

A suitable control strategy is vital to remove reference current to use shunt active filter effectively. Even though the p-q theory is effective, it exhibits synchronization problems with complicated calculations and transformations. The SRF theory is taken in this paper because of its dynamic behaviour. Another vital aspect of this work is to retain the voltage across the capacitor by means of ANN. Various theories and control strategies are discussed in the literature. $i_d - i_q$ Control scheme is introduced to reduce the harmonics and also retain DC-link potential achieved by means of various fuzzy membership functions [21,22]. DC-link potential is attained by Takagi–Sugeno-type controller with which the harmonics are mitigated [23]. The current harmonics as well as DC-link potentials are retained by means of an adaptive PI controller, as discussed in [24].

In this work, cascaded H-bridge MLI is employed as the control strategy for SAF, in which the harmonics are extracted by means of the synchronous reference frame theory-based CNN. The DC-link potential is retained by means of ANN classifier and then compared with that of proportional integral controller as well as fuzzy logic controller.

2. Proposed control methodology

In power distribution systems, the harmonics in the current and voltage increase mainly occur because of non-linear loads. Generally linear loads include resistive load and the non-linear loads include RL loads, RC loads and diode bridge rectifier loads. In non-linear loads, the harmonics in source current are generated and it is vital to mitigate these harmonics and hence a suitable methodology is proposed in this work, as shown in Figure 1.

When an AC supply is fed to a non-linear load, there are source current harmonics (I_{Sabc}). The reference current is generated by means of the Synchronous

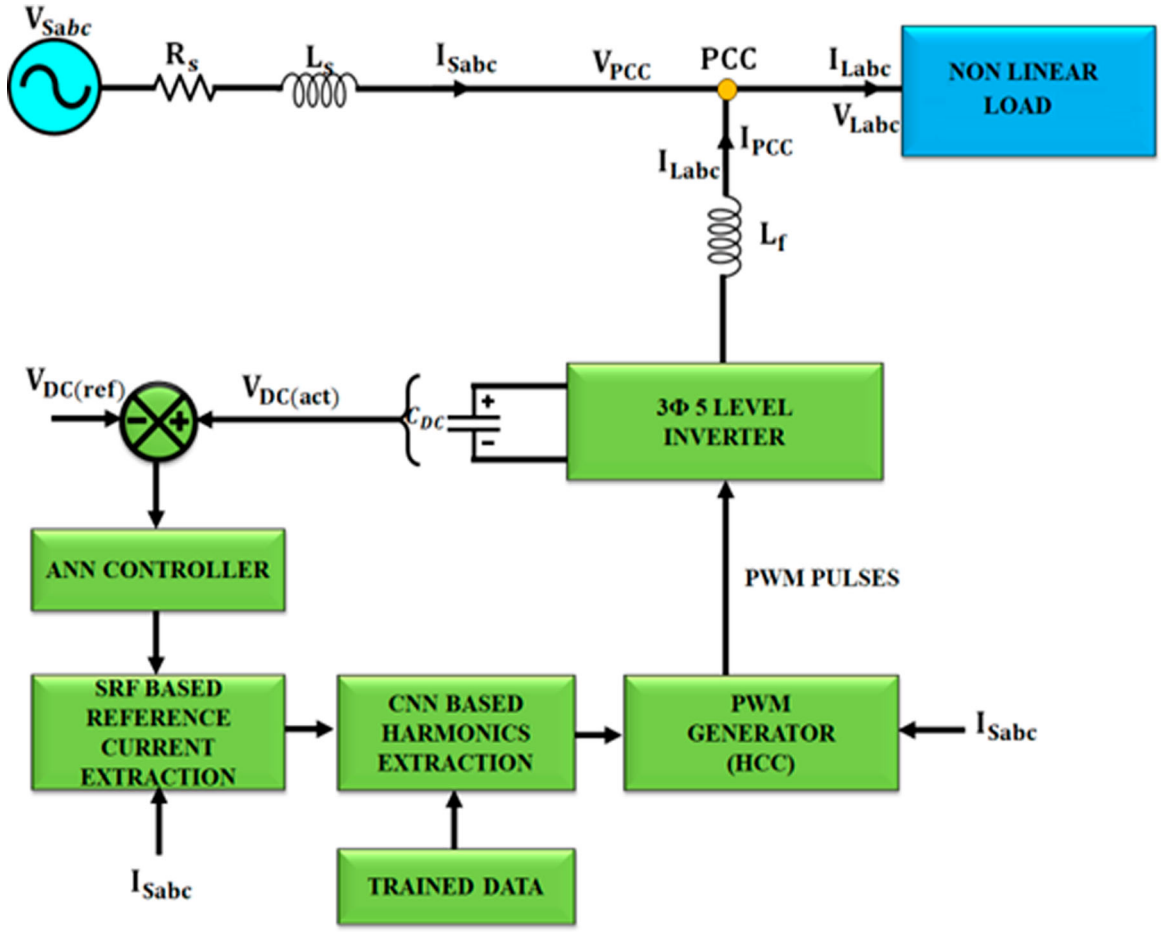

Figure 1. The proposed control methodology.

Reference Theory, which is one of the simplest reference current generation theories. By this theory, the pure current content is generated and further fed to the CNN classifier to extract the harmonics which is taken as the reference current which is given to pulse width modulation generator with HCC. To inject harmonics at PCC, a 5-level cascaded H-bridge inverter implemented on SAF is employed in this paper. Another vital part of this work is to maintain the DC-link potential. A reference of 1200 V is compared with the actual voltage V_{dc} which is then fed to the ANN classifier by which the efficiency and the robustness of the system increases. ANN is then compared with proportional integral controller & FLC which, in turn, reveals the effectiveness of ANN. The resultant thus attained from ANN is also fed to the SRF-based reference current generation unit. Now the output attained from CNN is fed to the PWM generator with HCC by which the gating sequence for 5-level inverter is generated. By using the 5-level inverter, total harmonic distortion is minimized. The outcome of the inverter is fed to the PCC by means of a coupling inductor. By this current and voltage, harmonics are eliminated in the source and a unity power factor is maintained, resulting in reactive power compensation.

The modelling of 5-level cascaded H-bridge inverter, SRF theory, CNN classifier, DC-link potential by means of proportional integral controller, Fuzzy controller as well as ANN are elaborated next .

3. Modelling of the proposed control methodology

3.1. Synchronous reference frame (SRF) theory

By means of the SRF theory [25], the reference current is generated. The SRF theory achieves steady-state and transient operations. It is preferred because of its simplicity and ease of calculation. The block diagram of SRF is depicted in Figure 2.

Here the transformation takes place from a 3φ stationary system to a 2φ rotating system. In the 3-phase system, the axes (a-b-c) are 120° apart from each other. These 3-phase frames are transformed to d-q axis rotating frames. Hence the current I_{Sa}, I_{Sb}, I_{Sc} are transformed to rotating coordinate current i_d-i_q.

$$i_d = \frac{2}{3}\left[I_{Sa}\sin\omega t + I_{Sb}\sin\left(\omega t - \frac{2\pi}{3}\right) + I_{Sc}\sin\left(\omega t + \frac{2\pi}{3}\right)\right] \quad (1)$$

$$i_q = \frac{2}{3}\left[I_{Sa}\cos\omega t + \mathrm{I}_{Sb}\cos\left(\omega t - \frac{2\pi}{3}\right) + I_{Sc}\cos\left(\omega t + \frac{2\pi}{3}\right)\right] \quad (2)$$

Based on the operation of PLL and currents, transformation takes place. The rotating speed of the phase-locked loop is set at the fundamental frequency ωt. $\sin\theta$and $\cos\theta$ is provided with phase-locked locked loop circuits. When the transformed currents (i_d, i_q) pass through the low-pass filter (LPF), the harmonics are filtered and only the fundamental components are allowed. The low-pass filter is designed on the basis of the Butterworth method with order 2. The difference in reference and actual value of DC-link potential fed to ANN retains DC-link potential of the capacitor. Now the components in d-q rotating frame are again transformed to a-b-c stationary frame. This can be attained by taking inverse transform and the resulting current equations in stationary reference frame are as follows:

$$I^*_{Sa} = i_d\sin\omega t + i_q\cos\omega t \quad (3)$$

$$I^*_{Sb} = i_d\sin\left(\omega t - \frac{2\pi}{3}\right) + i_q\cos\left(\omega t - \frac{2\pi}{3}\right) \quad (4)$$

$$I^*_{Sc} = i_d\sin\left(\omega t + \frac{2\pi}{3}\right) + i_q\cos\left(\omega t + \frac{2\pi}{3}\right) \quad (5)$$

The obtained reference current signals $(I^*_{Sa}, I^*_{Sb}, I^*_{Sc})$ are fed to the CNN classifier where the harmonics are further extracted.

3.2. Convolution neural network

The SRF theory is employed for generating the reference current and to further extract the harmonics, Convolutional Neural Network (CNN) is instigated in this paper. Here the detection of disturbances is carried out by means of IPCA (Improved Principal Component Analysis) [26] and the classification is carried out by means of one-dimensional CNN classifier.

3.2.1. IPCA

To extract the features PCA is used extensively in many applications. RMS, skewness, range, kurtosis, crest factor & form factor are statistical properties to be extracted while implementing IPCA. IPCA includes original data as well as Eigen vector (principal components) that minimizes the dimensions smoothly and also the time of computation in extracting the features. IPCA comprises the following three steps.

Step 1 – Forming Covariance matrix

Let Y_n be the training array of harmonics to be extracted which is given as $Y_n = [y_1, y_2, \ldots, y_n]^T \in \Re^N$ with length N. In IPCA the normalization of raw data takes place.

$$y'_{kl} = y_{kl}/\left(\frac{1}{n}\sum_{k=1}^{n} y_{kl}\right) \times (k = 1, 2, \ldots, n \text{ and } l = 1, 2, \ldots, m) \quad (6)$$

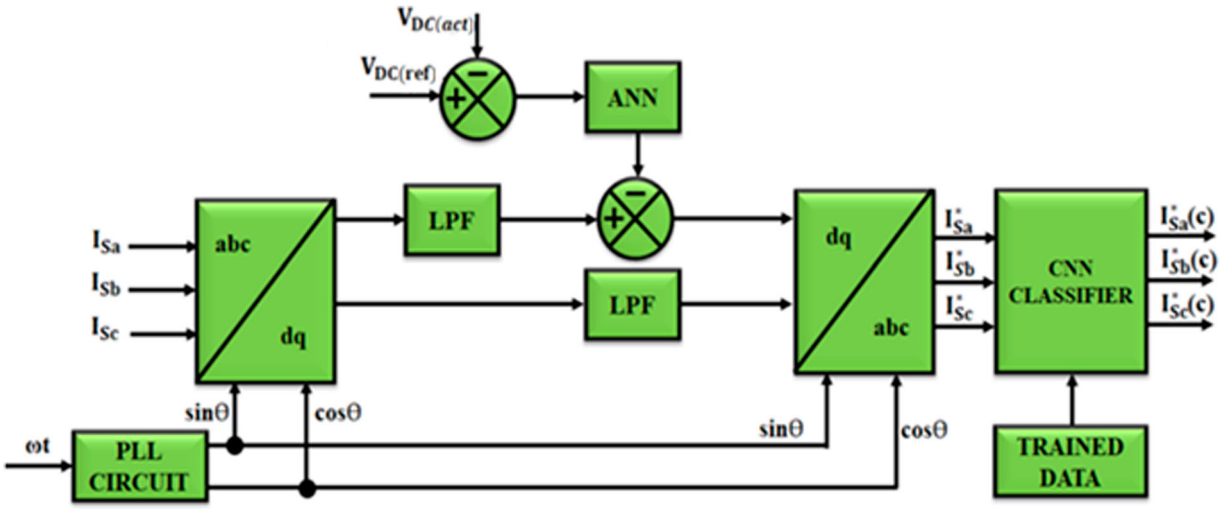

Figure 2. Reference current extraction from the SRF theory.

where y'_{kl} is the normalized value of y_{kl}, n and m represent the sample size and the number of dimensions, respectively. IPCA shows no loss of information. Covariance matrix can be expressed as follows:

$$C = \frac{1}{n}\sum_{i=1}^{n}[(y_{ik} - \overline{y_k}) - (y_{il} - \overline{y_l})] \tag{7}$$

Step 2 – Calculating Eigenvalue

By calculating the Eigenvalue the Covariance matrix is decomposed which can be represented as follows:

$$C = \sum_{x=1}^{N} \lambda_x A_x A_x^T = A \wedge A^T \tag{8}$$

where λ_x – Eigen value corresponding to the covariance matrix, A_x – Sub-Eigen values $[A_1, A_2, \ldots, A_x]$, x – Matrix rank, $\wedge$ – Diagonal matrix$[\lambda_1, \lambda_2, \ldots, \lambda_x]$, also $\lambda_1 > \lambda_2, \ldots \lambda_x$.

Step 3 – Calculating principal components

Once the covariance matrix is formed, eigenvalues and eigenvectors are calculated, the original data vector of M_n is transformed to uncorrelated vector z_n.

$$z_n = A^T M_n = \begin{bmatrix} a_{11}\, a_{12} \ldots a_{1m} \\ a_{21}\, a_{22} \ldots a_{2m} \\ \vdots \quad \vdots \quad \ddots \quad \vdots \\ a_{m1} a_{m2} \ldots a_{mm} \end{bmatrix}_{M \times M} \tag{9}$$

The data that are a proportion of the principal component n are included in the overall contribution rate η_n. To gather sufficient information η_n is set to 85%. The contribution rate η_k and the overall contribution rate η_n are determined by equations (10) and (11), respectively.

$$\eta_k = \left(\frac{\lambda_k}{\sum_{i=1}^{m} \lambda_i}\right) \times 100; (k = 1, 2, \ldots, m) \tag{10}$$

$$\eta_n = \sum_{k=1}^{n} \frac{\lambda_k}{\sum_{k=1}^{m} \lambda_k} > 85\% (i = 1, 2, \ldots, q) \tag{11}$$

After calculating the accurate values of n, principal components for R_k sample attain w_s:

$$R_k = \begin{bmatrix} R_{k1} \\ R_{k2} \\ \vdots \\ R_{kn} \end{bmatrix} = \begin{bmatrix} \delta_{11} & \delta_{21} & \ldots & \delta_{q1} \\ \delta_{12} & \delta_{22} & \ldots & \delta_{q2} \\ \vdots & \vdots & \ddots & \vdots \\ \delta_{1n} & \delta_{2n} & \ldots & \delta_{qn} \end{bmatrix} y_k^T \tag{12}$$

where $(i = 1,2, \ldots ,q)$.

3.2.2. CNN classifier

CNN classifier separates the harmonics accurately using the following features: mean, standard deviation, energy, entropy and log-energy entropy. CNN is basically a feed-forward network comprising three layers, namely, convolutional, maximum pooling and fully connected layers. It mainly extracts the features and its classification technique. The multilayer architecture of CNN is more complex, as it is vital to extract the features from each level. Here one-dimensional (1-D) CNN is taken for classifying the harmonics. In a two-dimensional CNN, there is a 2-D matrix, whereas in one-dimensional CNN it is replaced by means of the 1-D array. The illustration of the 1-D CNN is shown in Figure 3, which comprises convolution layer, network pooling layer and fully connected layer as well as the outer layer. The training of parameters is carried out by means of back propagation.

In the feature map, the pooling layer is considered as the down sampling layer which is down sampled by a factor of two and the largest value of this feature map is moved to the next layer. By this process, the number of training samples is improved, reducing the training time. This will be transferred to the next layer (fully connected) which includes several hidden layers. The pooled feature map as well as a fully connected network is linked by means of weights; the hidden and output layer and the final output classifier layer are interconnected. Forward propagation and back propagation are

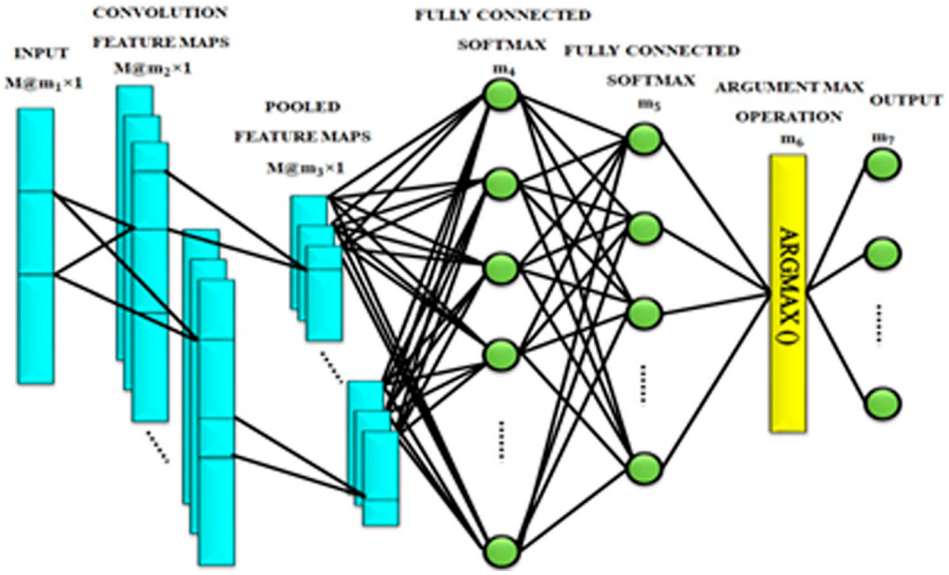

Figure 3. One-dimensional Convolution Neural Network.

the two steps of the training process in which the actual input data are provided by forward propagation and the upgrade of training parameters is provided by the back propagation. The representation of various layers is given as follows:

$$w_n^l = \sum_{i=1}^{M} w_i^{l-1} * j_{in}^l + b_n^l \tag{13}$$

where w_i^{l-1} is the previous $(l-1)^{\text{th}}$ layer's feature map; w_n^l is the current l^{th} layer's feature map; M – number of inputs; b_n^l additive bias of l^{th} layer; j is the number of Soft max units. The output is represented as follows:

$$z_n^l = f_n(w_n^l) \tag{14}$$

The Soft max layer is represented as

$$\delta(z)_n = \frac{e^{zn}}{\sum_j^J e^{z_j}}, n = 1, \ldots, J \tag{15}$$

The trainable parameters are updated using back propagation by means of the gradient descent scheme. To detect error, the output layer is interconnected with back propagation. Assume $l = 1$ as input layer & $l = \mathrm{L}$ as output layer where l is the number of classes, q is the input vector, $[z_1^I, \ldots, z_q^I]$ is the output vector and t_1^q is the target. Then the mean square error is given as follows:

$$E_q = \sum_{l=1}^{N_c} (z_l^I - t_l^q)^2 \tag{16}$$

IPCA minimizes the feature data which, in turn, minimize the computational load. Using all the input coefficients, the accuracy of classification will gets affected. Hence the selected coefficients, namely, mean (M), energy (E), standard deviation (SD), Entropy (ET), log-energy entropy (LE) are removed to minimize the complexity to enrich the classification accuracy. In this work, the number of kernels trained is a set of 50 and the number of three-phase waveforms obtained is 60. The expressions for principal components are given as follows:

Mean

$$M_{ki} = -\frac{1}{N} \sum_{j=1}^{N} X_{ij} \tag{17}$$

Energy

$$E_{ki} = \sum_{j=1}^{N} (|X_{ij}|^2) \tag{18}$$

Standard deviation

$$\sigma_{ki} = \left(\frac{1}{N} \sum_{j=1}^{N} (X_{ij} - \mu_i)^2 \right)^{\frac{1}{2}} \tag{19}$$

Entropy

$$ET_{ki} = -\sum_{j=1}^{N} X_{ij}^2 \log(X_{ij}^2) \tag{20}$$

Log-energy entropy

$$LE_{ki} = -\sum_{j=1}^{N} \log(X_{ij}^2) \tag{21}$$

In this work, the reference current signals $(I_{Sa}^*, I_{Sb}^*, I_{Sc}^*)$ obtained from the SRF theory are fed to the CNN classifier by which the harmonics are further minimized and the resultant reference current $(I_{Sa}^*(c), I_{Sb}^*(c), I_{Sc}^*(c))$ is given to pulse width modulation generator as HCC generates required gating pulses to five-level inverter.

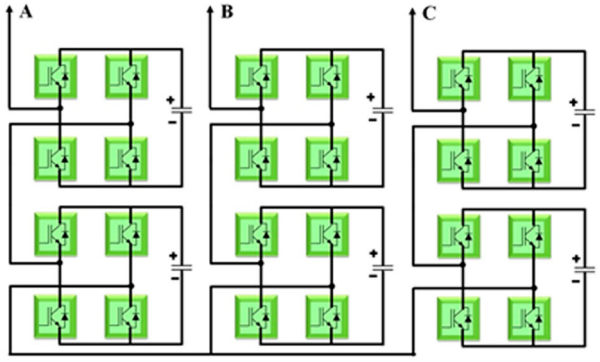

Figure 4. Cascaded H-bridge five-level inverter.

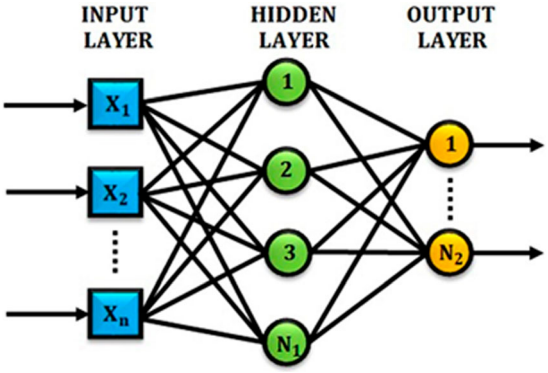

Figure 5. Artificial Neural Network.

4. Cascaded H-bridge five-level inverter

A cascaded H-bridge 5-level inverter-based SAF is employed for the harmonic mitigation. The schematic depiction of 3Φ five-level inverter is depicted in Figure 4 which is designed based on H-bridge topology. The merit of cascaded multi-level inverters is its ease of control and modularity.

The inverter is designed in such a way that it has 2 H-bridges for every phase in cascaded with 24 IGBTs and a separate capacitor is provided for each H-bridge, which is meant for storing energy. ANN classifier is to retain DC-link potential. The phase potential of cascaded H-bridge multi-level inverter is given as the sum of voltages of individual H-bridges. The switching sequence for the IGBTs is attained from the PWM generator with Hysteresis Current Controller (HCC).

5. Control of DC-link voltage

For proper working of SAF, it is more vital that DC-link potential is retained constant and for this reason, it is vital to monitor the active power flowing through the SAF. If the filter losses and the active power monitored were equal, then V_{DC} can be retained. The oscillations in V_{DC} are mainly for the capacitor losses and for the delay in the control circuit. Hence to retain the DC-link potential, ANN is employed. The behaviour of ANN is compared with those of PI controller & FLC.

5.1. PI controller

The actual and reference values of V_{DC} are compared and given to the PI controller. Hence the reference current is acquired from proportional integral controller; error and transfer function are given in equation (22) and (23), respectively. Thus, the output attained from the PI controller is the active current necessary to retain V_{DC} which compensates the power loss that occurs inside the filter.

$$e = V_{dc,ref} - V_{dc} \tag{22}$$

$$H(S) = K_p + \frac{K_i}{s} \tag{23}$$

where K_p is the proportional gain and K_i is the integral gain. As there exists a maximum peak overshoot problem in the PI controller, there is a problem with the settling time also. So dc-link voltage is controlled with the help of the Fuzzy controller.

5.2. Fuzzy controller

To attain better dynamic responses, intelligent controllers are employed nowadays. Here the PI controller is compared with Fuzzy controller which makes the system more efficient than the proportional integral controller. A FLC comprises fuzzification, rule base and defuzzification. The error along with change in error is computed and fed as input to FLC (here, error along with change in error is taken from reference as well as actual values of DC-link voltage). The normal values are transformed to fuzzy values in the fuzzification process. By considering the rules and its membership functions, data interpretation is performed in the rule base section. In defuzzification, the fuzzified values are converted to normal data. And by this DC-link potential is kept almost constant.

For retaining DC-link potential and to further reduce THD, Artificial Neural Network is implemented in this paper by which the overall system performance is improved.

5.3. Artificial Neural Networks (ANN)

The principle of artificial intelligence is to enable the system to decide and to learn from the experience. ANN mimics the biological neural network in which

Table 1. Design parameters.

Parameters	Values
System frequency	50 Hz
Line-line source voltage	440 V
Source resistor (R_s)	1 Ω
Source inductor (L_s)	0.1 mH
DC-side capacitance (C_{DC})	2100 μF
Reference voltage ($V_{DC(ref)}$)	1000 V
Coupling inductor (L_f)	1 mH

the control is made through machines or systems. The general architecture of ANN given in Figure 5 includes an input layer, a hidden layer as well as an output layer. The input to ANN is provided by means of the input layer which is then forwarded to the middle layer.

The weight that connects the input layer and the hidden layer is multiplied with the input. Based on the bias applied to the hidden layers, computations are performed and are processed in the output layer. Among the various architectures and learning rules for ANN,

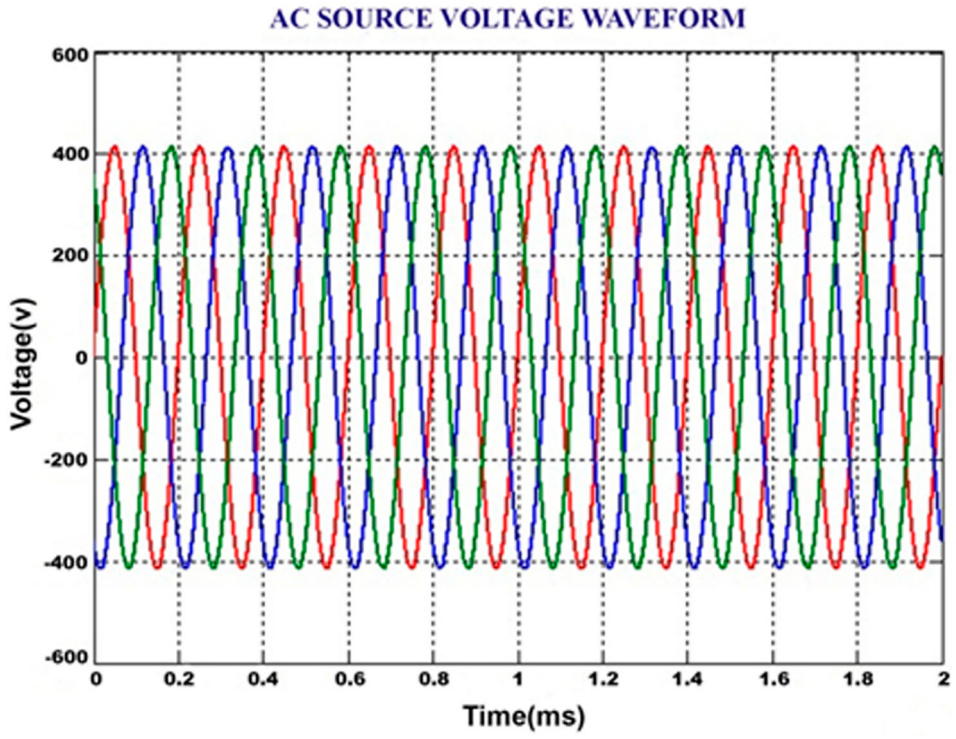

Figure 6. Source voltage waveform.

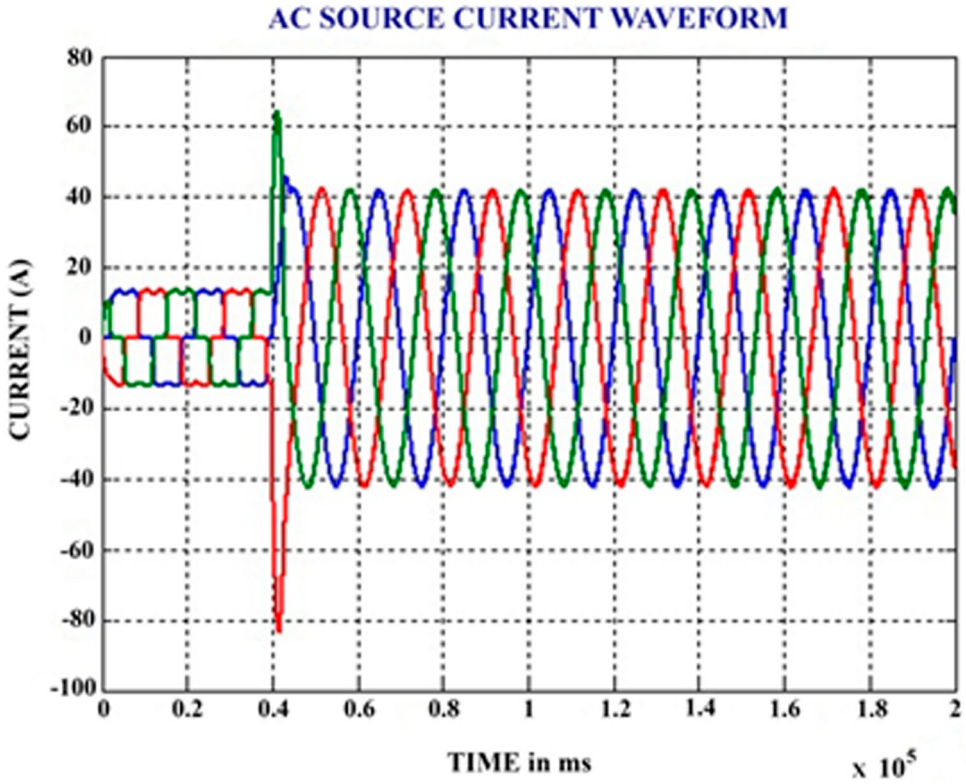

Figure 7. Source current waveform.

feed-forward back propagation is well suited for many power electronic applications [27]. Here the weights are updated and the procedure is repeated for new weights until the desired target is met. To get faster convergence, the LMBP (Levenberg–Marquardt Back propagation) training method is instigated.

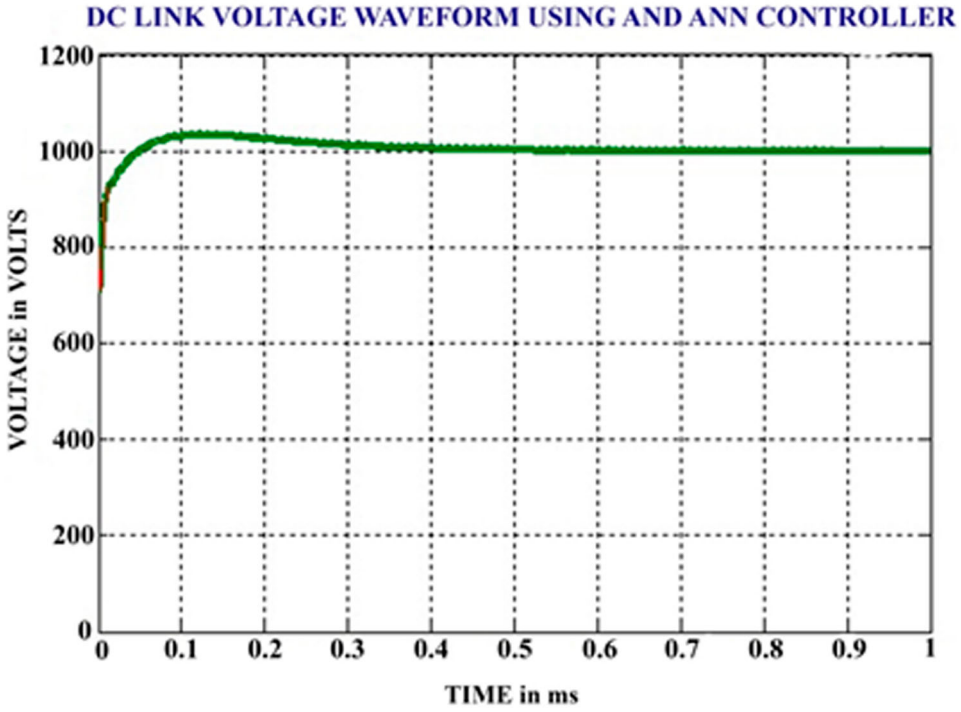

Figure 8. DC-link voltage with ANN controller.

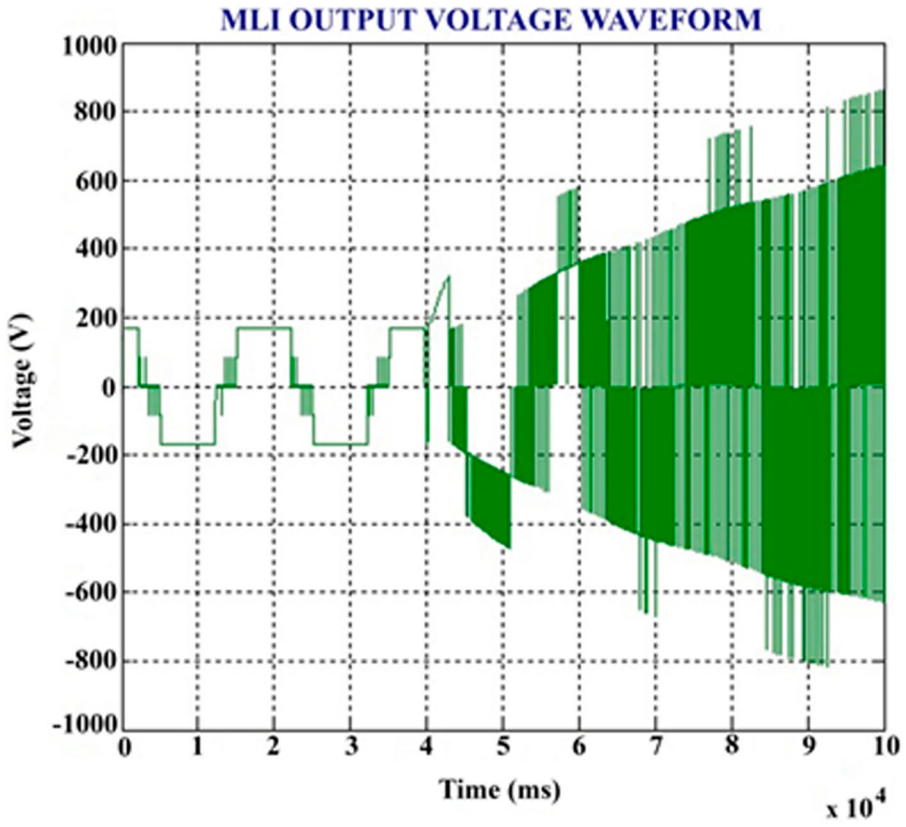

Figure 9. Five-level inverter output.

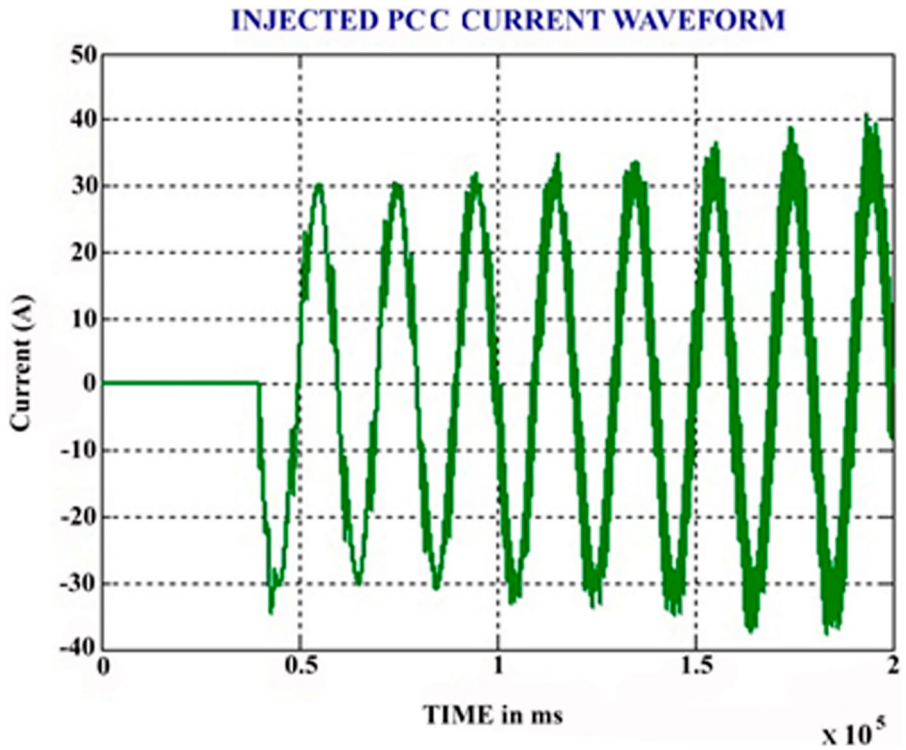

Figure 10. Current waveform injected to PCC.

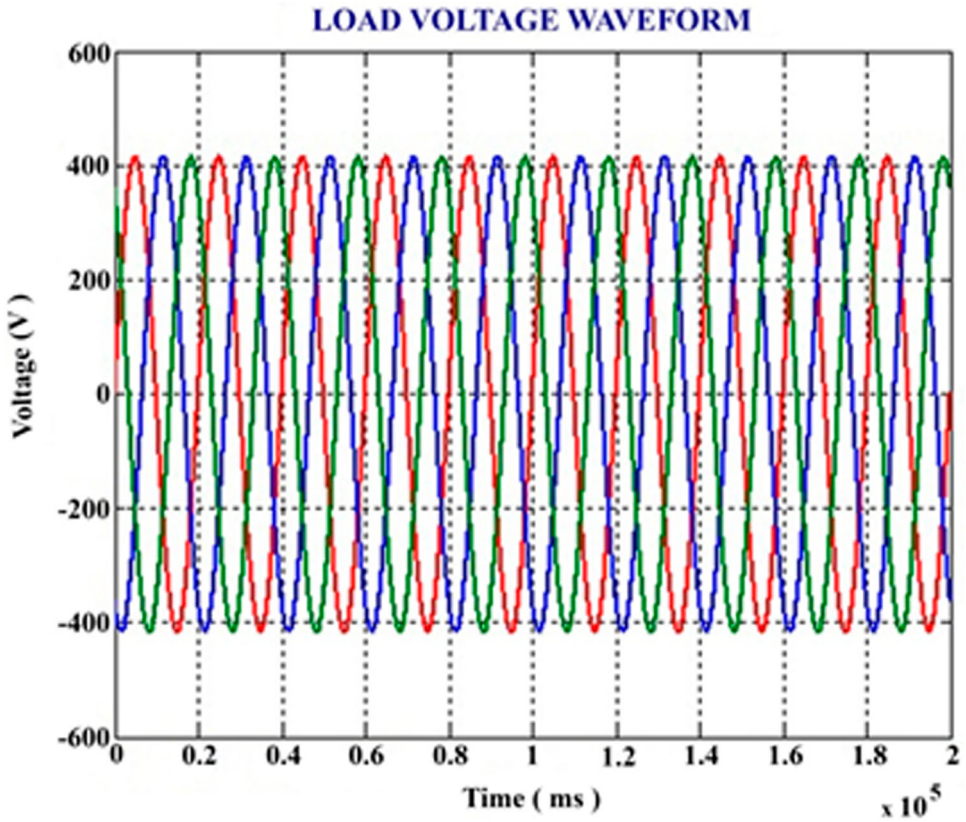

Figure 11. Load voltage waveform.

Here ANN is implemented for retaining DC-link potential of the capacitor. It comprises 100 hidden layers and LMBP algorithms are implemented for training the network.

6. Observed results and discussions

The proposed control methodology is analysed through simulation in MATLAB and in hardware using FPGA Spartan 6E. The harmonic reduction is achieved by

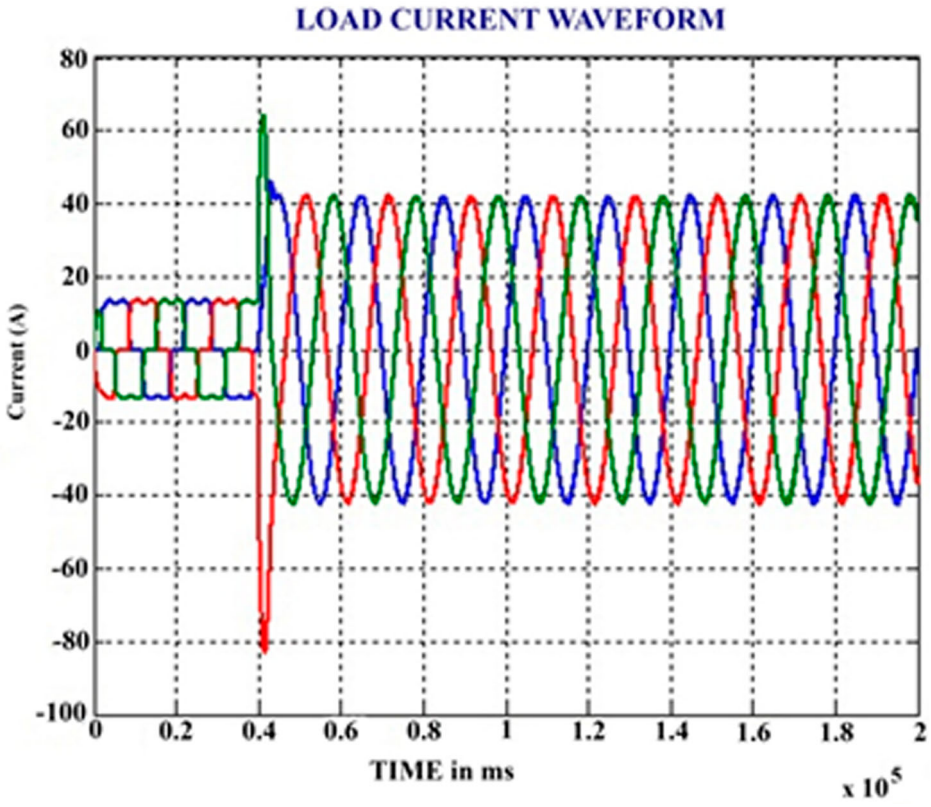

Figure 12. Load current waveform.

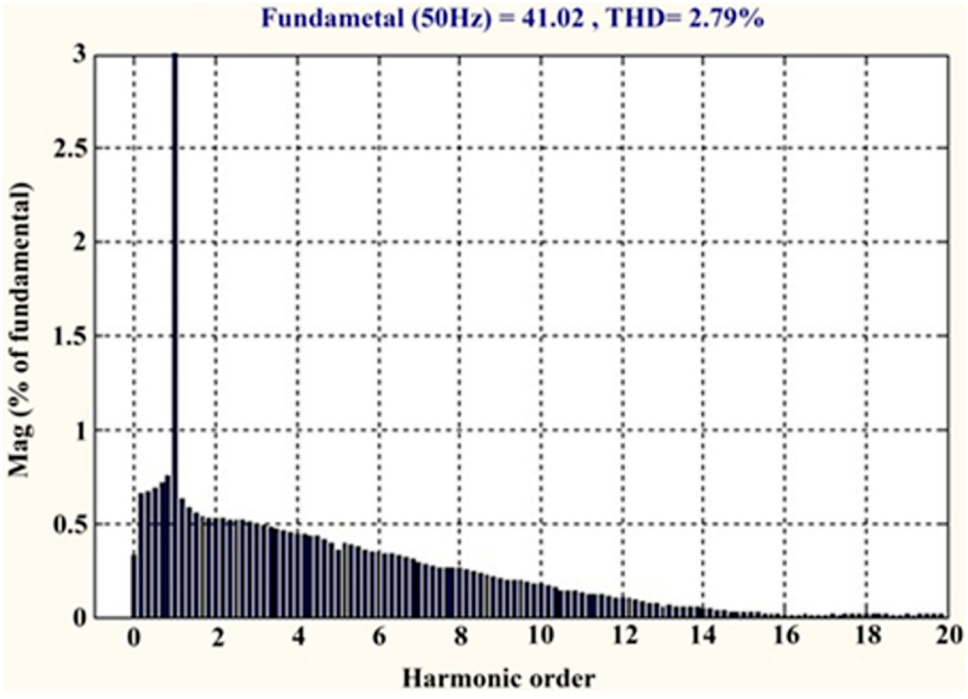

Figure 13. Source current THD with SRF.

means of the SRF theory with CNN also the DC-link voltage is retained. The parameters used for the simulation are given in Table 1.

The simulated result of source voltage and the source current waveforms are depicted in Figures 6 and 7, respectively. A voltage of 415 V is maintained. When this voltage is applied to a non-linear load, initially there are harmonics in the source current and it was found that after 0.04 ms the waveform becomes sinusoidal due to the use of SAF. The source voltage cannot

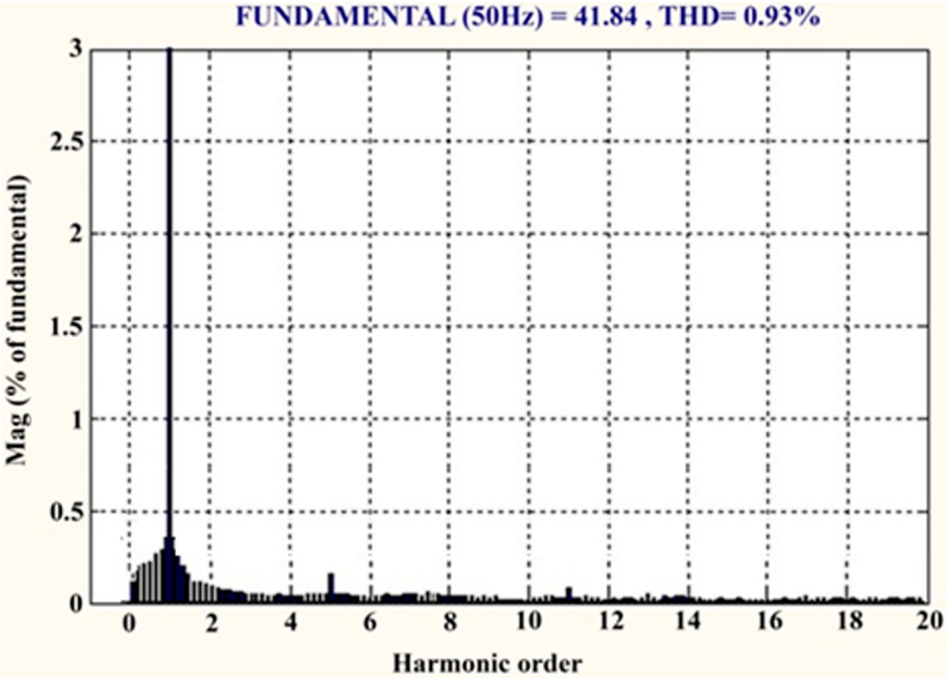

Figure 14. Source current THD with CNN.

be controlled directly, but the effect of THD in source current reflects in the source voltage which makes the voltage waveform sinusoidal.

The DC-link voltage waveform using ANN controller is depicted in Figure 8 from which it is observed that the waveform settles around 0.35 s. The inverter's output waveform is shown in Figure 9. This output is then passed through the coupling inductor and the filter current, as shown in Figure 10, is injected to the PCC. The amplitude of inverter current is the same as the source current but the phase components are opposite to eliminate the harmonics in the source current.

Table 2 indicates ANN is superior to Fuzzy and PI controllers in controlling the dc-link voltage.

The load voltage and load current waveforms are shown in Figures 11 and 12, respectively. It is depicted from the load current waveform that there are harmonics in the initial stage and after 0.04 ms the waveform becomes sinusoidal.

Figure 13 shows the source current THD of 2.79% with the SRF theory. And this can be further minimized by incorporating CNN classifier and THD of 0.93% is attained, as shown in Figure 14.

Table 2. Performance comparison of ANN with Fuzzy and PI controllers.

Controller	K_p	K_I	(t_r)	(t_p)	(t_s)	e_{ss}
PI controller	0.293	13.35	0.283	0.361	0.377	0.34
Fuzzy controller	0.375	32.18	0.242	0.294	0.315	0.27
ANN controller	0.328	26.44	0.103	0.158	0.173	0.15

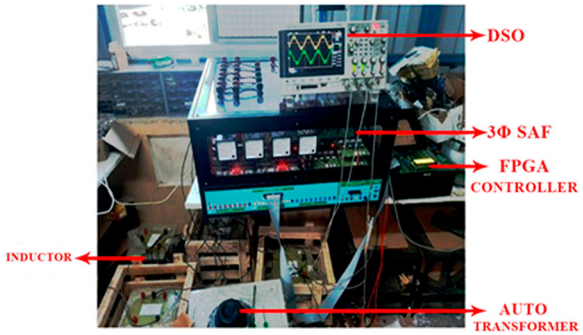

Figure 15. Hardware set-up.

6.1. Hardware implementation

The proposed control methodology can also be implemented in hardware using FPGA Spartan 6E and the hardware set-up is shown in Figure 15.

Figure 16 shows the source voltage, source current, PCC and inverter output waveforms attained from the experimental set-up. Three-phase waveforms are shown in Figure 16(a), and (b) shows the waveforms for single-phase. From the waveforms, it is depicted that there are oscillations in the initial stage after that the waveforms become sinusoidal.

Figure 17 shows the load voltage and load current waveforms and it is observed that even though the load voltage and load current show oscillations, the source voltage and current waveforms (Figure 16) show reduced harmonics. The load current representation for all the three phases is shown in Figure 18 and it is depicted that the harmonics are reduced and the load current is made sinusoidal (Figure 19).

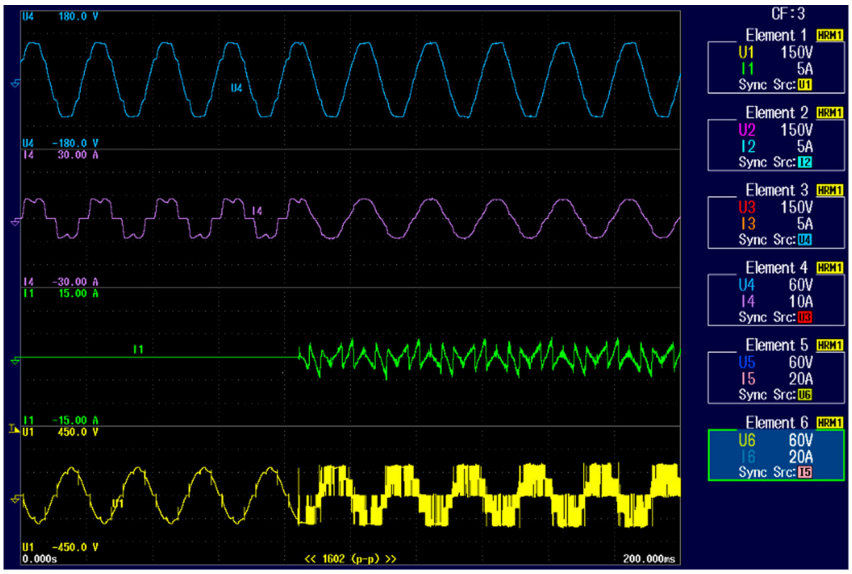

(a)

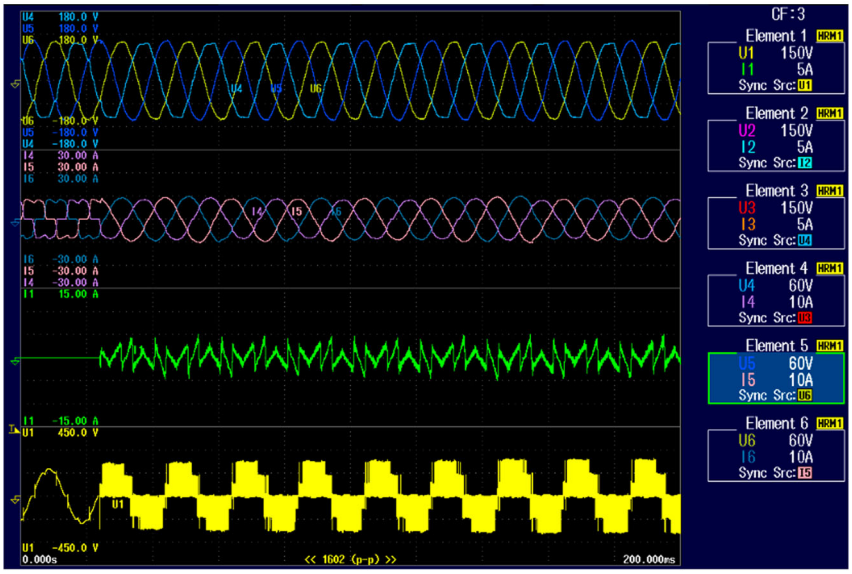

(b)

Figure 16. Waveforms for source voltage, source current, PCC and inverter output (a) Single phase, (b) Three phase.

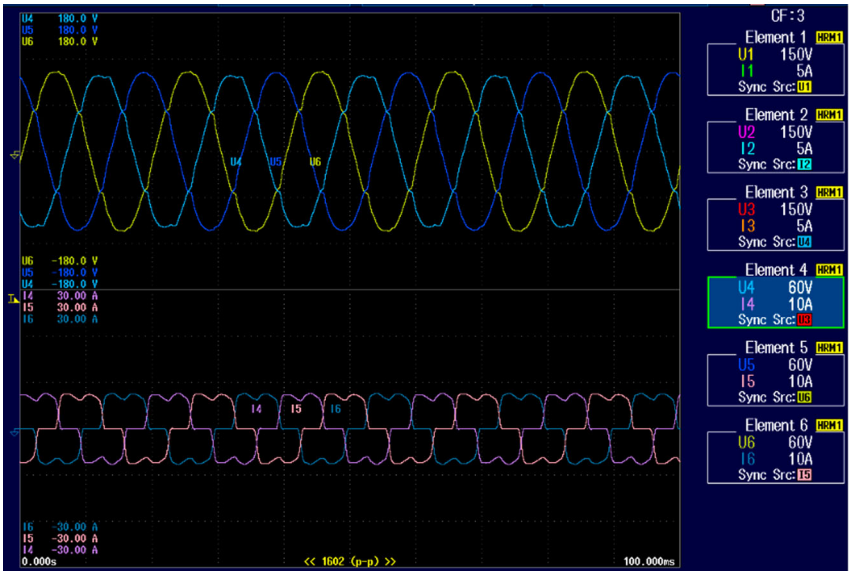

Figure 17. Load voltage and load current waveforms.

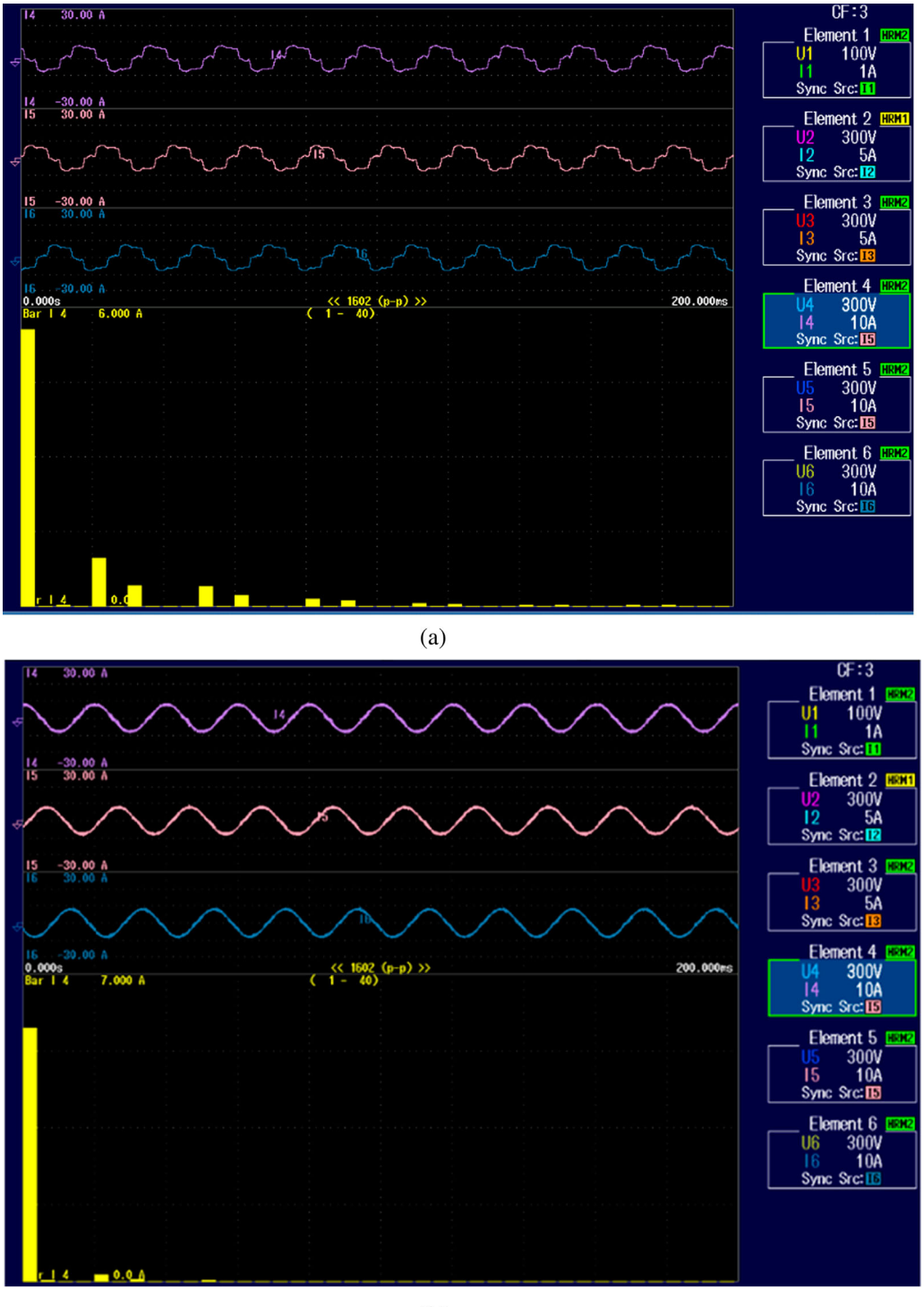

Figure 18. Load current waveforms (a) Before compensation (b) After compensation.

The representation of the source current THD is given in Figure 20. From Figure 20(a) it is depicted that the THD of 4.168% is attained by implementing SRF and it is further minimized by the CNN classifier which is 1.4%, as shown in Figure 20(b).

7. Conclusion

In this work, a framework of the Synchronous Reference Theory with CNN classifier implemented to mitigate harmonics with reactive power compensation and retaining DC-link voltage is carried out. The reference current generation is done with the SRF theory, and the harmonic extraction is done by means of CNN classifier. For retaining the DC-link voltage, ANN is incorporated for comparison with proportional integral controller and FLC. The gating sequence for the five-level inverter is generated by the PWM generator-incorporated HCC. Thus, the harmonics are reduced in a three-phase system for nonlinear loads. From the

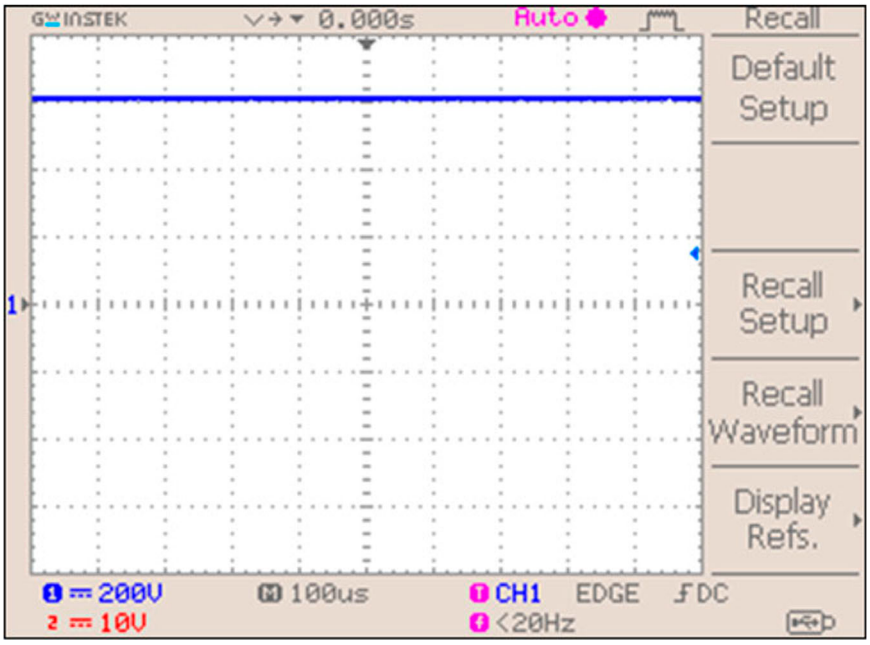

Figure 19. DC-link voltage waveform.

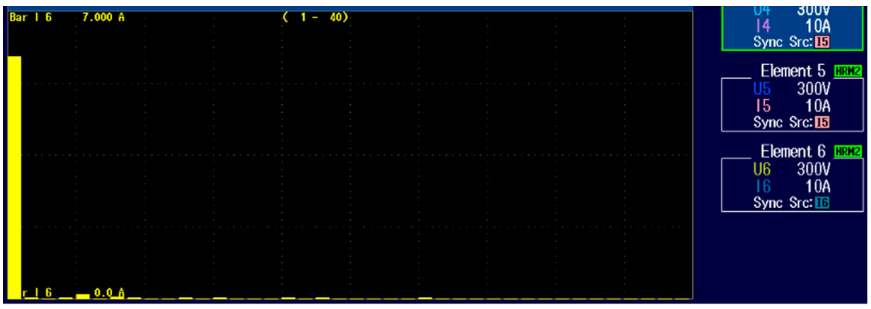

(a)

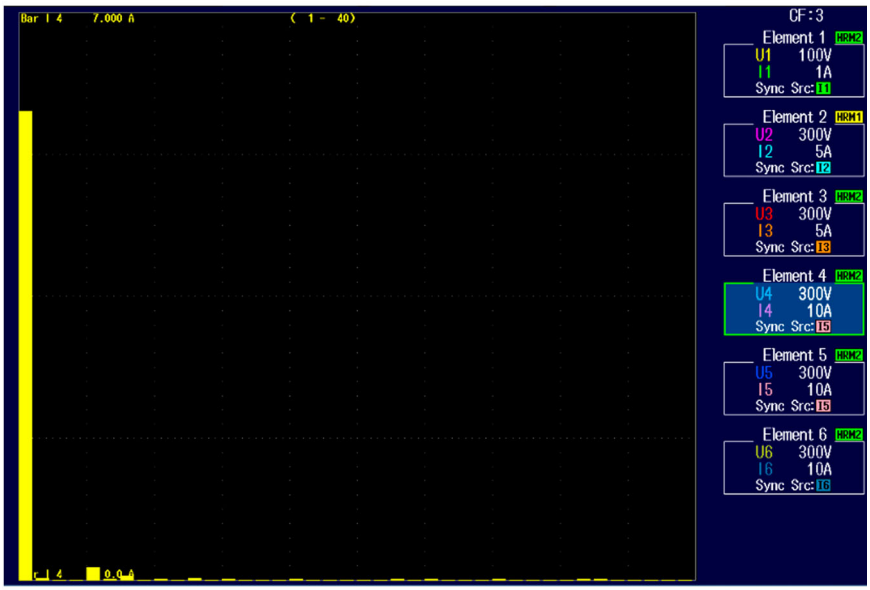

(b)

Figure 20. Representation of THD (a) SRF (b) ANN.

simulation results, it is observed that the THD of 0.93% and THD of 1.4% are achieved in hardware execution process. The DC-link voltage is retained with a settling time of around 0.35seconds. Thus, the proposed control methodology reveals that it is more efficient in reducing the harmonics.

Disclosure statement

No potential conflict of interest was reported by the author(s).

ORCID

K. R. Sugavanam http://orcid.org/0000-0003-3872-0938

References

[1] Harmonics PS. Power system harmonics: an overview. IEEE Trans Power Appar Syst. 1983;102(8):2455–2460.
[2] Stones J, Collinson A. Power quality. Power Eng J. 2001;15(2):58–64.
[3] Milanovic JV, Zhang Y. Global minimization of financial losses due to voltage sags with FACTS based devices. IEEE Trans Power Delivery. 2010;25(1):298–306.
[4] Zhang Y, Milanović JV. Global voltage sag mitigation with FACTS-based devices. IEEE Trans Power Deliv. 2010;25(4):2842–2850.
[5] Liao H, Milanović JV. On capability of different FACTS devices to mitigate a range of power quality phenomena. IET Gener Transm Distrib. 2017;11(5):1202–1211.
[6] Singh B, Al-Haddad K, Chandra A. A review of active filters for power quality improvement. IEEE Trans Ind Electron. 1999;46(5):960–971.
[7] El-Habrouk M, Darwish MK, Mehta P. Active power filters: a review. IEE Proc Electr Power Appl. 2000;147(5):403–413.
[8] Jintakosonwit P, Akagi H, Fujita H, et al. Implementation and performance of automatic gain adjustment in a shunt-active filter for harmonic damping throughout a power distribution system. IEEE Trans Power Electron. 2002;17(3):438–447.
[9] Tey LH, So PL, Chu YC. Improvement of power quality using adaptive shunt active filter. IEEE Trans Power Deliv. 2005;20(2):1558–1568.
[10] Longhui W, Fang Z, Pengbo Z, et al. Study on the influence of supply-voltage fluctuation on shunt active power filter. IEEE Trans Power Deliv. 2007;22(3):1743–1749.
[11] Kanjiya P, Khadkikar V, Zeineldin HH. Optimal control of shunt active power filter to meet IEEE std. 519 current harmonic constraints under non-ideal supply condition. IEEE Trans Ind Electron. 2015;62(2):724–734.
[12] Ray PK. Power quality improvement using VLLMS based adaptive shunt active filter. CPSS Trans Power Electron Appl. 2018;3(2):154–162.
[13] Wang Y, Xu J, Feng L, et al. A novel hybrid modular three-level shunt active power filter. IEEE Trans Power Electron. 2018;33(9):7591–7600.
[14] Tareen WUK, Mekhielf S. Three-phase transformerless shunt active power filter with reduced switch count for harmonic compensation in grid-connected applications. IEEE Trans Power Electron. 2018;33(6):4868–4881.
[15] Corzine K, Familiant Y. A new cascaded multilevel H-bridge drive. IEEE Trans Power Electron. 2002;17(1):125–131.
[16] Dian R, Xu W, Mu C. Improved negative sequence current detection and control strategy for H-bridge three-level active power filter. IEEE Trans Appl Supercond. 2016;26(7):0611905.
[17] Masaoud A, Ping HW, Mekhilef S, et al. Novel configuration for multilevel DC-link three-phase five-level inverter. IET Power Electron. 2014;7(12):3052–3061.
[18] Salem A, Ahmed EM, Orabi M, et al. New three-phase symmetrical multilevel voltage source inverter. IEEE J Emerg Sel Top Circ Sys. 2015;5(3):430–442.
[19] Nguyen MK, Tran TT. Quasi cascaded H-bridge five-level boost inverter. IEEE Trans Ind Electron. 2017;64(11):8525–8533.
[20] Rao BN, Suresh Y, Panda AK, et al. Development of cascaded multilevel inverter based active power filter with reduced transformers. CPSS Trans Power Electron Appl. 2020;5(2):147–157.
[21] Mikkili S, Panda AK. Simulation and real-time implementation of shunt active filter ID-IQ control strategy for mitigation of harmonics with different fuzzy membership functions. IET Power Electron. 2012;5(9):1856–1872.
[22] Mikkili S, Panda AK. Types-1 and -2 fuzzy logic controllers-based shunt active filter Id-Iq control strategy with different fuzzy membership functions for power quality improvement using RTDS hardware. IET Power Electron. 2013;6(4):818–833.
[23] Honkanen J, Hannonen J, Korhonen J, et al. Nonlinear PI-control approach for improving the DC-link voltage control performance of a power-factor-corrected system. IEEE Trans Ind Electron. 2019;66(7):5456–5464.
[24] Merai M, Naouar MW, Slama-Belkhodja I, et al. An adaptive PI controller design for DC-link voltage control of single-phase grid-connected converters. IEEE Trans Ind Electron. 2019;66(8):6241–6249.
[25] Kumar SK, Ranga J, Kumar CSP, et al. PV based shunt active power filter for harmonics mitigation using decoupled DSRF theory. IEEE International Conference on Advanced Computing & Communication Systems (ICACCS); 2019: 1108–1110.
[26] Shen Y, Abubakar M, Liu H, et al. Power quality disturbance monitoring and classification based on improved PCA and convolution neural network for wind-grid distribution systems. Energies. 2019;12(7):1280.
[27] Iqbal M, Jawad M, Jaffery MH, et al. Neural networks based shunt hybrid active power filter for harmonic elimination. IEEE Access. 2021;9:69913–69925.